JACS
JOURNAL OF THE AMERICAN CHEMICAL SOCIETY
Communication
pubs.acs.org/JACS

Spontaneous Partition of Carbon Nanotubes in Polymer-Modified Aqueous Phases

Constantine Y Khripin, Jeffrey A. Fagan, and Ming Zheng*

Materials Science and Engineering Division, National Institute of Standards and Technology, 100 Bureau Drive, Gaithersburg, Maryland 20899, United States

Supporting Information

ABSTRACT: The distribution of nanoparticles in different aqueous environments is a fundamental problem underlying a number of processes, ranging from biomedical applications of nanoparticles to their effects on the environment, health, and safety. Here, we study distribution of carbon nanotubes (CNTs) in two immiscible aqueous phases formed by the addition of polyethylene glycol (PEG) and dextran. This well-defined model system exhibits a strikingly robust phenomenon: CNTs spontaneously partition between the PEG- and the dextran-rich phases according to nanotube's diameter and metallicity. Thermodynamic analysis suggests that this chirality-dependent partition is determined by nanotube's intrinsic hydrophobicity and reveals two distinct regimes in hydrophobicity-chirality relation: a small diameter (<1 nm) regime, where curvature effect makes larger diameter tubes more hydrophobic than small diameter ones, and a large diameter (>1.2 nm) regime, where nanotube's polarizability renders semiconducting tubes more hydrophobic than metallic ones. These findings reveal a general rule governing CNT behaviors in aqueous phase and provide an extremely simple way to achieve spatial separation of CNTs by their electronic structures.

Many studies have focused on how chemical functionalities grafted or adsorbed on the surface of nanoparticles affect their distribution in aqueous phases.[1,2] However, fewer studies are directed toward defining the roles of intrinsic atomic and electronic structures of nanoparticles in their interactions with aqueous environment. Recently, we initiated an investigation of colloidal carbon nanotubes (CNTs) in aqueous solution crowded by polymers. This study led to the finding that crowding polymers can exert an entropy-driven depletion force to induce length-dependent CNT cluster formation.[3] While length is the dominant physical dimension of a CNT, it is the CNT chirality that defines its atomic and electronic structure and thereby determines its physical/chemical properties.[4] We noticed in our early study that the crowding induced CNT clustering process could be chirality selective when certain polymers were chosen. This triggered a search for optimal conditions to observe chirality-dependent CNT behavior in aqueous solutions and eventually led us to test aqueous two-phase polymer systems[5] for sensitively monitoring chirality-dependent effects.

Figure 1a shows our experimental design: two water-soluble polymers, polyethylene glycol (PEG) and dextran, are chosen for our experiments. When concentrations of the two polymers are at ≈6 w/w %, two separate phases are formed with the PEG-rich and more hydrophobic phase at the top and the dextran-rich and more hydrophilic phase at the bottom. The difference in hydrophobicity between the two phases can be precisely tuned by controlling concentrations of the two polymers.[5,6] CNTs used in the experiment are dispersed in sodium cholate (SC). When a CNT dispersion is mixed with the two polymers and appropriate amount of sodium dodecyl sulfate (SDS) (see Supporting Information (SI) for more experimental details), spontaneous and robust CNT partition

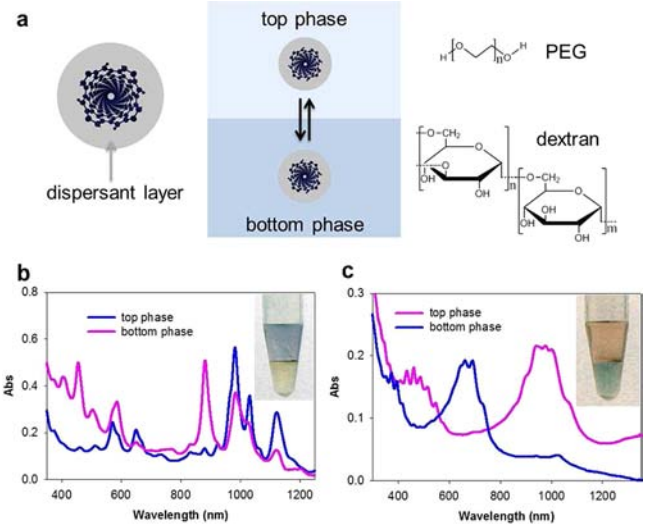

Figure 1. Spontaneous partition of CNTs in PEG/dextran two-phase system. (a) Schematics of the two-phase system used in this study. Top phase is PEG-rich, and bottom phase is dextran-rich. (b) Partition of small diameter CoMoCAT tubes. (c) Partition of large diameter arc-discharge tubes. In both cases, CNTs were prepurified by ultracentrifugation and length sorted by size-exclusion chromatography. UV−vis near IR absorption spectra from the top (pink trace) and bottom (blue trace) phase are shown. Inset in each panel shows the measured sample. Average length is 150 nm for the CoMoCAT and 220 nm for the arc-discharge sample. Further experimental details are given in the SI.

Received: March 18, 2013
Published: April 22, 2013

dx.doi.org/10.1021/ja402762e | J. Am. Chem. Soc. 2013, 135, 6822−6825

in the two separated polymer phases is observed. Systematic investigation reveals two regimes of partition behaviors according to nanotube's diameter. For small diameter (0.6−1.0 nm) nanotubes represented by the CoMoCAT synthetic mixture, we observe clear diameter-based partition (Figure 1b); smaller diameter tubes, such as (6,4), are in the more hydrophilic dextran-rich phase, whereas larger diameter (7,5) and (8,4) tubes are in the more hydrophobic PEG-rich phase. For large diameter (1.2−1.5 nm) tubes made by the arc-discharge method, we observe clean metallic/semiconductor separation (Figure 1c). Metallic tubes are partitioned in the more hydrophilic dextran-rich phase, and semiconducting tubes are in the more hydrophobic PEG-rich phase.

The partition-based separation can be easily scaled up in CNT concentration and volume. Partition readily occurs at all possible CNT concentrations tested up to 1 mg/mL with similar separation resolution. Figure 2a shows a few test samples with CNT concentrations up to 0.1 mg/mL, beyond which the interphase boundary is difficult to visualize due to strong optical absorption by CNTs. Figure 2b shows a partition experiment done in 1 L volume, demonstrating the feasibility of volume scale-up. It is also possible to repeat CNT partition multiple times to dramatically improve the purity of CNT fractions of interest. Figure 2c shows the result of a four-step partition experiment, in which the semiconductor enriched fraction in the top PEG-rich phase is used as the starting material for the next round of partition. It is remarkable that after three rounds of partition, metallic absorption features become nondetectable.

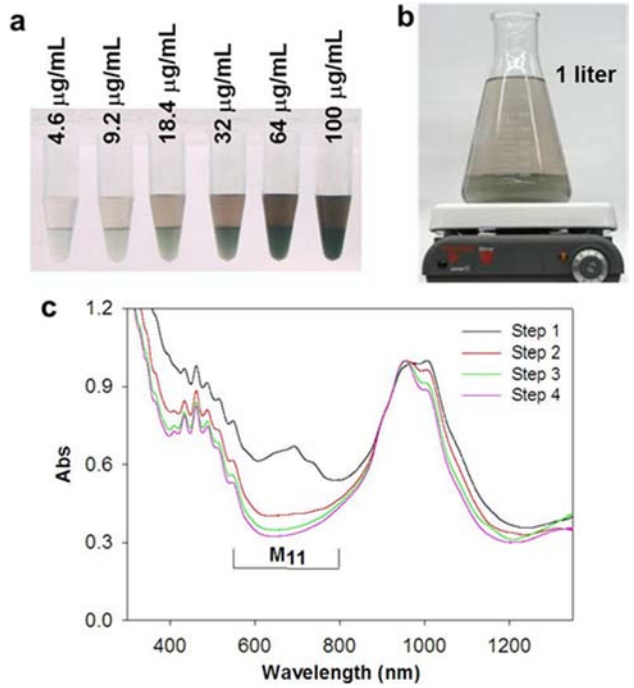

Figure 2. Concentration/volume scaling and repeated CNT partition. (a) Image of partition samples with increasing amount of CNT loading from left to right. (b) A 1 L volume partition sample. (c) UV−vis near IR spectra of semiconducting CNT fractions obtained from four steps of repeated partition. Spectra are rescaled for easy comparison. Absorption features in the M_{11} region (550−800 nm) from the metallic CNTs are dramatically reduced in the sample from step two relative to that from step one and become nondetectable in samples from steps three and four. As dispersed arc-discharge tubes were used in these experiments. Other conditions are the same as given in Figure 1. For reasons not clear at the moment, we often observe that 5−10% of CNTs are trapped at the interface.

We find that CNT partition in the two-phase system can be conveniently tuned by a number of factors, including nanotube length, surfactant and chaotropic salt concentrations, and temperature. To illustrate this, we have determined partition coefficient $K = C_t/C_b$, the ratio between CNT number concentration in the top phase (C_t) and the bottom phase (C_b), for metallic and semiconductor arc-discharge tubes under a variety of conditions. Figure S1 summarizes the trends we have observed.

In what follows, we apply thermodynamics to analyze the observed partition phenomena. Partition is driven by thermodynamic equilibrium of colloidal CNTs in two different phases. The equilibrium condition requires that chemical potentials of nanotubes in the top and bottom phases are equal. This gives the expression for the partition coefficient I (assuming dilute concentration limit):

$$K = \frac{C_t}{C_b} = \exp\left(-\frac{\mu_t^0 - \mu_b^0}{kT}\right) \quad (1)$$

In eq 1, μ_t^0 and μ_b^0 are standard chemical potentials of CNTs in the top and bottom phases, respectively, k is Boltzmann constant, and T is absolute temperature. Eq 1 reveals the origin of the sensitivity of our experimental system: The difference in CNT/polymer interaction in the two phases is exponentially amplified to yield difference in the CNT populations. Given the 1D nature of a CNT, it is reasonable to propose[6] that the standard chemical potential of a given nanotube chirality, (n,m), in an aqueous polymer solution can be written as

$$\mu^0 = \bar{\mu}(n, m)A + \mu_e \quad (2)$$

where $\bar{\mu}(n,m)$ is the standard chemical potential per unit sidewall area, A is the sidewall area of the nanotube, and μ_e accounts for contributions from the nanotube ends, which contain most likely carboxylate and hydroxyl functionalities. The chirality-dependent partition originates from the $\bar{\mu}(n,m)$ term in eq 2. It is determined by the CNT and surfactant coating structures as well as surfactant and polymer compositions in the two phases. To simplify our analysis, we consider the case where surfactant/CNT binding is not strong (relative to kT), resulting in residual bare CNT surface not covered by the surfactant. This is what has been reported for SDS-coated CNTs.[7] If we set the solvation free energy for the fully surfactant-coated CNT as the zero reference level, denote s as the fraction of bare CNT surface not covered by surfactants, and $\overline{\Delta G}(n,m)$ as the solvation free energy per unit area (or per unit carbon atoms) of the bare and intrinsically hydrophobic CNT, then to a first approximation

$$\bar{\mu}(n, m) = s\overline{\Delta G}(n, m) \quad (3)$$

Combining eqs 1−3, we obtain

$$\ln K = (s_b - s_t)\left[\frac{\overline{\Delta G}(n, m)}{kT}\right]A + \frac{\mu_{e,b} - \mu_{e,t}}{kT} \quad (4)$$

where subscript b and t denote parameters for the bottom and top phases, respectively.

Eq 4 connects each CNT's partition coefficient with its intrinsic hydrophobicity as measured by $\overline{\Delta G}(n,m)$. For nanotubes of different diameters, their relative degree of

dx.doi.org/10.1021/ja402762e | J. Am. Chem. Soc. 2013, 135, 6822−6825

hydrophobicity can be predicted based on the general trend established for globular hydrophobic molecules.[8] It has been shown that the solvation free energy per unit area for a hydrophobic sphere increases linearly with its diameter in the small diameter (<1 nm) regime, beyond which the solvation energy reaches to a plateau value corresponding to the surface tension of water−vapor interface.[8] The physics behind this trend, which is that small hydrophobic objects merely reorder hydrogen bonds, whereas large ones break hydrogen bonds and create liquid−vapor interface,[8] should also hold for CNTs. Based on this reasoning, we plot in Figure 3a the expected

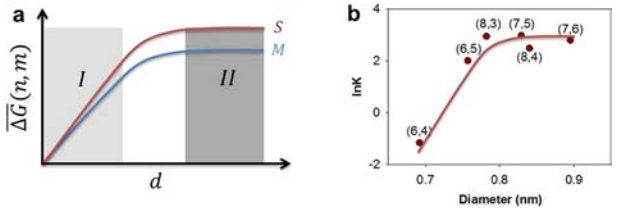

Figure 3. Two regimes of partition behavior. (a) CNT hydrophobicity plot showing expected CNT solvation energy per unit area $\overline{\Delta G}(n,m)$ as a function of diameter and metallicity. In the small diameter regime I, $\overline{\Delta G}(n,m)$ is proportional to diameter; in the large diameter regime II, $\overline{\Delta G}(n,m)$ becomes independent of diameter but dependent on metallicity. (b) Experimentally determined partition coefficient for semiconducting tubes vs diameter. The smooth curve is just a guide to show the trend. A sample similar to the one used in Figure 1b were measured by fluorescence spectroscopy to determine partition coefficient for each (n,m) species.

trend for $\overline{\Delta G}(n,m)$. Note that the curve for metallic tubes is below that for semiconducting tubes, this is because metallic tubes are more polarizable and thus expected to be more hydrophilic than semiconducting tubes.[9]

Analysis of CNT partition data in light of eq 4 suggests that the $\overline{\Delta G}(n,m)$ trend plotted in Figure 3A is the main source of the observed two distinct regimes of chirality-dependent CNT partition: In the small diameter regime (I), the difference in $\overline{\Delta G}(n,m)$ between two diameter tubes overwhelms that between metallic and semiconducting tubes, leading to mainly diameter-based partition; in the large diameter regime (II), the opposite is true, resulting in mainly metal/semiconductor separation. Using fluorescence spectroscopy, we have determined partition coefficients for a set of semiconducting CNTs of different diameters (Figure 3b). The similar trend shown in Figure 3a,b strongly suggests that partition trend is mainly determined by $\overline{\Delta G}(n,m)$. The fact that we observe mainly metallic and semiconducting tube separation for large diameter arc-discharge tubes (Figure 1c) lends further support to the dominant role played by $\overline{\Delta G}(n,m)$.

We now consider partition trends shown in Figure S1. The effect of surfactant concentration and composition on partition are captured by the scaling factors in eqs 3 and 4. Our experiments show that the weak surfactant SDS is required for good separation. This is rationalized in our analysis as a condition for eq 3. At fixed SDS:SC ratio, when the overall surfactant concentration is low, colloidal CNTs are expected to be more hydrophobic due to more exposed bare CNT surface, making them more stable in the slightly more hydrophobic PEG-rich phase ($(s_b - s_t) > 0$), the opposite is true when surfactant concentrations are high. These are consistent with our observations as shown in Figure S1b. Next, higher temperatures would result in desorption of surfactant from the nanotube surface, resulting in greater exposure of hydrophobic areas and partition into the PEG-rich phase (Figure S1d). Nanotube length is proportional to sidewall area A and should play a role according to eq 4, but its effect is convoluted with that of chirality and the ends, resulting in less clear-cut partition trend as a function of length. Slower diffusion rate for longer nanotubes[10] may also kinetically limit their partition coefficients given by eq 4. Nevertheless, using length-sorted arc-discharge tube fractions for metallic/semiconducting tube partition, we do observe clear length effect as shown in Figure S1a. Finally, the chaotropic salt NaSCN, but not the kosmotropic salt Na_2SO_4, pushes colloidal CNTs into the bottom dextran-rich phase (Figure S1c), presumably due to its ability to reduce the solvation energy more in the bottom phase than in the top phase.[11]

We suggest that the hydrophobicity plot (Figure 3a) provides a common physical basis for many different separation mechanisms.[12−23] Among numerous separation schemes reported, liquid chromatography (LC)[12,14−17,20,21] and density-gradient ultracentrifugation (DGU)[19,22,23] are the two leading methods that have demonstrated clear chirality-based separation. In the case of various LC methods, separation relies on chirality-dependent CNT partition between a more hydrophobic stationary phase and more hydrophilic mobile phase. Retention time, which is linearly dependent on the partition coefficient,[24] typically follows this order: small diameter tubes < large diameter tubes and metallic tubes < semiconductor tubes,[14−16] consistent with the hydrophobicity plot. In the case of DGU, separation is enabled by the chirality-dependent effective density, which in large part is determined by the surfactant and hydration layers, which ultimately are governed by the hydrophobicity−chirality relation. This explains why in the DGU method diameter sorting is more effective for small diameter tubes, and metal/semiconductor sorting is more readily achieved for large diameter tubes.[19] Furthermore, it is intriguing that the mixed surfactant composition originally mapped out by Arnold et al.[19] appears to be a common condition for separating surfactant dispersed CNTs in all of the separation approaches discussed here. This is again suggestive that modulating CNT's intrinsic hydrophobicity to achieve chirality differentiation is the common theme of these separation approaches.

Our findings provide a much more effective way to separate CNT by chirality. We note that mechanistically CNT partition is coupled with the polymer phase separation dynamics: during the initial mixing step, (n,m)-dependent interactions lead to separation of CNTs into two disordered, bicontinuous polymer phases of microscopic dimension, which then coalesce to form macroscopic separation.[25] The entire process is thermodynamically downhill, spontaneous and fast, driven by internal molecular forces. In contrast, in the case of LC, differential partition of CNTs in the stationary and mobile phases has to be converted into temporal separation of the CNTs by an external flow field; in the case of DGU, the chirality-dependent effective density differences give rise to macroscopic spatial separation only under ultrahigh centrifugal acceleration over several hours. Both LC and DGU require sophisticated instrumentations to implement. The partition method, on the other hand, is simple and fast, consumes minimal amount of energy, and requires no major instrumentation. These advantages make our method especially suited for multistep sorting to obtain high-purity metallic, semiconducting, and even single-chirality tubes.

dx.doi.org/10.1021/ja402762e | J. Am. Chem. Soc. 2013, 135, 6822−6825

Progress along this direction is underway and will be reported in our future publications.

Our observation is a clear demonstration of electronic structure-dependent nanoparticle distribution in aqueous phases. We have tested other water-soluble polymer pairs (e.g., polyvinylpyrrolidone/dextran) and other colloidal CNTs (e.g., DNA-wrapped CNTs) and observed similar CNT partitioning, suggesting that CNT structure-based partition in polymer phases is a general phenomenon. It is likely that other colloidal nanoparticle systems also exhibit partition phenomena in aqueous phases. This has implications in the biodistribution of nanoparticles.[26] Finally, we note that the CNT partition phenomenon can be used in conjunction with many well-developed polymer phase engineering techniques to achieve controlled spatial assembly of CNTs by their electronic structures. A possible use of such assembly is for energy conversion, as demonstrated by a recent study.[27] Technological applications employing electronic structure-based partition of nanoparticles in polymer phases are waiting to be explored.

■ ASSOCIATED CONTENT

Ⓢ Supporting Information

Figures and experimental details. This material is available free of charge via the Internet at http://pubs.acs.org.

■ AUTHOR INFORMATION

Corresponding Author

ming.zheng@nist.gov

Notes

The authors declare no competing financial interest.

■ ACKNOWLEDGMENTS

We thank Drs. Anand Jagota, Kalman Migler, and Jack Douglas for their critical comments on the manuscript. We would also like to thank Yuri Khripin and Irina Nazarenko for useful suggestions with respect to aqueous biphasic systems.

■ REFERENCES

(1) Monopoli, M. P.; Aberg, C.; Salvati, A.; Dawson, K. A. *Nat. Nanotechnol.* **2012**, *7*, 779.

(2) Balazs, A. C.; Emrick, T.; Russell, T. P. *Science* **2006**, *314*, 1107.

(3) Khripin, C. Y.; Arnold-Medabalimi, N.; Zheng, M. *ACS Nano* **2011**, *5*, 8258.

(4) Saito, R.; Dresselhaus, G.; Dresselhaus, M. S. *Physical Properties of Carbon Nanotubes*; Imperial College Press: London, 1998.

(5) Albertsson, P.-A. *Partition of Cell Particles and Macromoleucles*, 2nd ed.; Wiley-Interscience: Hoboken, NJ, 1971.

(6) Zaslavsky, B. Y. *Aqueous Two-Phase Partitioning*; Marcel Dekker: New York, 1994.

(7) Niyogi, S.; Densmore, C. G.; Doorn, S. K. *J. Am. Chem. Soc.* **2008**, *131*, 1144.

(8) Chandler, D. *Nature* **2005**, *437*, 640.

(9) Bresme, F.; Wynveen, A. *J. Chem. Phys.* **2007**, *126*, 044501.

(10) Tsyboulski, D. A.; Bachilo, S. M.; Kolomeisky, A. B.; Weisman, R. B. *ACS Nano* **2008**, *2*, 1770.

(11) Lo Nostro, P.; Ninham, B. W. *Chem. Rev.* **2012**, *112*, 2286.

(12) Moshammer, K.; Hennrich, F.; Kappes, M. *Nano Res.* **2009**, *2*, 599.

(13) Hirano, A.; Tanaka, T.; Kataura, H. *ACS Nano* **2012**, *6*, 10195.

(14) Liu, H.; Nishide, D.; Tanaka, T.; Kataura, H. *Nat. Commun.* **2011**, *2*, 309.

(15) Liu, H.; Feng, Y.; Tanaka, T.; Urabe, Y.; Kataura, H. *J. Phys. Chem. C* **2010**, *114*, 9270.

(16) Tu, X.; Manohar, S.; Jagota, A.; Zheng, M. *Nature* **2009**, *460*, 250.

(17) Tanaka, T.; Jin, H.; Miyata, Y.; Fujii, S.; Suga, H.; Naitoh, Y.; Minari, T.; Miyadera, T.; Tsukagoshi, K.; Kataura, H. *Nano Lett.* **2009**, *9*, 1497.

(18) Tu, X.; Zheng, M. *Nano Res.* **2008**, *1*, 185.

(19) Arnold, M. S.; Green, A. A.; Hulvat, J. F.; Stupp, S. I.; Hersam, M. C. *Nat. Nanotechnol.* **2006**, *1*, 60.

(20) Zheng, M.; Jagota, A.; Strano, M. S.; Santos, A. P.; Barone, P.; Chou, S. G.; Diner, B. A.; Dresselhaus, M. S.; McLean, R. S.; Onoa, G. B.; Samsonidze, G. G.; Semke, E. D.; Usrey, M.; Walls, D. J. *Science* **2003**, *302*, 1545.

(21) Zheng, M.; Jagota, A.; Semke, E. D.; Diner, B. A.; McLean, R. S.; Lustig, S. R.; Richardson, R. E.; Tassi, N. G. *Nat. Mater.* **2003**, *2*, 338.

(22) Tyler, T. P.; Shastry, T. A.; Leever, B. J.; Hersam, M. C. *Adv. Mater.* **2012**, *24*, 4765.

(23) Green, A. A.; Hersam, M. C. *Adv. Mater.* **2011**, *23*, 2185.

(24) Giddings, J. C. *Unified Separation Science*; John Wiley & Sons, Inc.: Hoboken, NJ, 1991.

(25) Bates, F. S. *Science* **1991**, *251*, 898.

(26) Clegg, J. S. *Am. J. Physiol.* **1984**, *246*, R133.

(27) Han, J.-H.; Paulus, G. L. C.; Maruyama, R.; Heller, D. A.; Kim, W.-J.; Barone, P. W.; Lee, C. Y.; Choi, J. H.; Ham, M.-H.; Song, C.; Fantini, C.; Strano, M. S. *Nat. Mater.* **2010**, *9*, 833.